Research Article / Araştırma Makalesi GU J Sci, Part A, 9(3): 233-250 (2022) https://doi.org/10.54287/gujsa.1135609

Gazi University
Journal of Science
PART A: ENGINEERING AND INNOVATION
http://dergipark.org.tr/gujsa

Optimal Cutting Conditions of Abrasive Waterjet Cutting for Ti-6Al-2Sn-2Mo Alpha-Beta Alloy Using EDAS and DFA Methods

Ugochukwu Sixtus NWANKITI[1*], Sunday Ayoola OKE[1]

[1]*Department of Mechanical Engineering, University of Lagos, Lagos, Nigeria*

Keywords

Abrasive Machining
Waterjet
Optimization
Metal Alloys
EDAS
DFA

Abstract

Abrasive waterjet machining (AWJM), a known metal cutting process in manufacturing, is likely to be improved with the selection and use of the most influential parameters in machining decision-making. This work illustrates the development of two multicriteria indicators to optimize parameters for the abrasive waterjet machining process, providing optimization information for the surface morphology problem. The evaluation based on the distance from average solution (EDAS) method was used as the first indicator while the desirability function analysis (DFA) method reflects the second indicator. The results demonstrate a huge promise of both indicators, EDAS and DFA, to develop procedures for optimizing the parameters of Ti-6Al-2Sn-4Zr-2Mo alpha-beta alloy through the abrasive waterjet machining process. For the EDAS method, experimental trial 7 provided the best results with the water jet pressure of 220 bar, traverse speed of 40mm/min, and standoff distance of 1mm. The corresponding material removal rate is 151.667mm3/min while the roughness average is 2.76mm. The DFA method also provided the same results as those of the EDAS method. The present study is evidence of optimization of the parameters of Ti-6Al-2Sn-4Zr-2Mo alpha-beta alloy using the AWJM process. This warrants an intervention to enhance productivity and the economic gains of the company.

Cite

Nwankiti, U. S., & Oke, S. A. (2022). Optimal Cutting Conditions of Abrasive Waterjet Cutting for Ti-6Al-2Sn-2Mo Alpha-Beta Alloy Using EDAS and DFA Methods.*GU J Sci, Part A, 9*(3), 233-250.

Author ID (ORCID Number)

U. S. Nwankiti, 0000-0003-4186-9346
S. A. Oke, 0000-0002-0914-8146

Article Process

Submission Date 27.06.2022
Revision Date 09.08.2022
Accepted Date 11.08.2022
Published Date 26.09.2022

1. INTRODUCTION

Waterjet machining (WJM) represents a modern, innovative process utilizing a non-conventional machining procedure, stimulated by a water stream propelled in high rapidity (Akkurt, 2004; Ergür, 2009; Hashish, 2014; Kartal, 2017; Karakurt et al., 2019). It is an alternative to the conventional metal subtraction methods of grinding and milling but with extraordinary impact in removing substantial materials from the surface of the material in rapid successions beyond the limits of the grinding and milling methods (Kartal, 2017; Karakurt et al., 2019). Besides, it displaces the conventional cutting method of hacksawing for some precision jobs where the surface finished by hacksawing is unacceptable by standards as the abrasive waterjet machine can cut the metals into two parts. The WJM is versatile and able to process plastics, rubber or walls where the convectional hacksawing or CNC cutting process has limitations. However, as abrasive material is used in machining, like metals and granite and embedded in the water, for the machining process, abrasive waterjet machining (AWJM) is a more appropriate term.

The AWJM process borrows from the principle of water erosion, which explains that as high-velocity water strikes the surface of a metal, material removal results (Karakurt et al., 2019; Wang et al., 2021). Depending on the softness or hardness of the material being cut, the choice of water is made (Sitek et al., 2021). While pure water has been involved in transforming the surfaces of soft materials, it is challenging to use it for cutting harder materials. This is done by mixing the water with abrasives (Singh et al., 2021). As abrasive

*Corresponding Author, e-mail: sa_oke@yahoo.com

particles are mixed with the water for the surface transformation of the Ti-6Al-25n-4Zr-2Mo alpha-beta alloy being considered here, the name abrasive waterjet machining emerges (Singh et al., 2021; Sitek et al., 2021). In practice, aluminium oxide, garnet, glass beads and sand are the largest commonly used abrasives. Furthermore, the Ti-6Al-25n-4Zr-2Mo alpha-beta stated above is referred to as near alpha titanium alloy. They are chosen in this article because of their suitability to build equipment and their components that are subjected to high temperatures and loads (Marya & Edwards, 2002; Bhamare et al., 2013). The wide applicability of the alloy includes jet engines, boilers, ovens and gas turbines. The Ti-6Al-25n-4Zr-2Mo (Ti-6-2-4-2) alloy is a preferred choice because of its remarkable strength-to-weight ratios, corrosion resistance, low Young's modulus and outstanding creep resistance.

However, research has proved that in different processes, the Ti-6Al-25n-4Zr-2Mo alloy can be optimised. For instance, in the laser shock peening process, the bending fatigue life of the Ti-6Al-25n-4Zr-2Mo alloy was enhanced by Bhamare et al. (2013). The authors concluded that the obtained optimal parametric set form thickness compression yielded an extensive enhancement of the bending fatigue life for the laser powder bed fusion process where the optimization of post-process heat treatments is the concern, Fleißner-Rieger et al. (2022) in utilising the Ti-6Al-25n-4Zr-2Mo (Ti-6-2-4-2) alloy concluded as follows. The authors declared that the optimization approach led to the alloy exhibiting optimized ductility and substantial growth of elongation at fracture. Moreover, Perumal et al. (2022) concluded that applying the wire electrical discharge machining to Ti-6242 (Ti-6Al-25n-4Zr-2Mo) alloy at testing at optimal situations yields enhanced material removal rate and acceptable surface finish. Likewise, Marya and Edwards (2002) concluded that in a laser bending optimization process using Ti-6Al-25n-4Zr-2Mo alloy, bending was achieved at an utmost value of roughly 0.65 of the melting temperature. Also, Perumal et al. (2021) declared that optimising the Ti-6Al-25n-4Zr-2Mo alloy in wire electrical discharge machining process using the analysis of variance showed the superior necessary parameters for surface roughness to be a pulse on time, pulse off time as well as a fused pulse on time and pulse off time, revealing contributions by the percentage of 22.71% and 36.88%, correspondingly.

In all the above studies, it is common to have applied the Ti-6Al-25n-4Zr-2Mo alloy in non-conventional processes and this is done to enhance the mechanical properties of the material such as tensile strength of 1110MPa, yield strength of 1050MPa, Poisson's ratio of 0.325, and an elastic modulus of 118GPa. The non-convectional systems process of difficult-to-machine materials is possible to be made by conventional machining. Furthermore, the inference from all these studies is that the Ti-6Al-25n-4Zr-2Mo alloy is an important material, which may be exploited by various processes. It is added that enormous processes and methods are still not being exploited. Thus the use of other optimization methods to enhance process parameters is a gap to be exploited. As much as the authors are aware, previous studies have failed to tackle the complex analysis and tedious information processing that may exist while attempting to optimize the abrasive waterjet machining parameters of Ti-6Al-25n-4Zr-2Mo alloy but also in selecting the most important AJWM process parameters form the multiple options feasible while still optimizing the parameters. Although solving the complexity and tedious information processing is the main issue of attaining high efficiency in the AWJM process a single characteristic assures that the process engineer diverts attention to the most important parameters in the process.

While justifying the necessity for more studies on the parametric predictions of the AWJM, Ergur (2009) argued that the paucity of knowledge that explains the hydraulic attributes of AWJM limits the understanding and expansion of the process control and optimization domain of the AWJM. Consequently, studies on optimization modelling and multicriteria analysis applied to abrasive waterjet machining have been fruitful in the previous years (Muthuramalingam et al., 2018; Perec and Musial, 2021). For example, Perec and Musial (2021) revealed the performance of the Hardox steel machined through the abrasive waterjet process on the application of multicriteria approach of entropy/VIKOR with the focus parameters as the cut kerf angle, abrasive flow rate over the cutting depth, pressure, cut surface roughness and feed rate. The method was declared feasible in this instance. Notwithstanding the complication of the approach while considering multiple parameters is an issue of concern. On the other hand, Muthuramelingan et al. (2021) applied the Taguchi-data envelopment analysis-oriented ranking using a multiresponse decision-making approach to improve responses that include material removal rate and surface roughness. It was concluded that standoff distance impacts energy in the greatest form for the abrasive waterjet machining process.

Besides, Perec et al. (2021) proposed the optimization of the hardox steel during the abrasive waterjet cutting procedure. The feasibility of the approach using the combined grey relational analysis and Taguchi method was confirmed. Miao et al. (2018) deployed multipass abrasive waterjet cutting to process the AISI 304 stainless steel. The optimization cutting turns to process the AISI 304 stainless steel were determined. Zohoor and Nourian (2012) deployed an algorithm to optimize the abrasive waterjet machining process using an experimental approach. It was concluded that the transverse speed and nozzle parameters impacting on the response, which is geometry kerf quality.

In Iqbal et al. (2011) the optimization of the abrasive jet process parameters was conducted on the AISI 4340 steel and aluminium 2219 using the analysis of variance as the tool of optimization to concurrently maximise various integrations of performance indices. Besides, Chen et al. (2019) eliminated shape errors at the external corners of the material. They declared that jet lag is the principal reason causing the bump error while the slow involve traversing speed causes overcut. While correcting those errors, the authors, ascertained that a bump removal angle and an approach to complete optimal length for the lead-in/lead-out lines were proposed for the respective errors of bump error and overcut. In another study, Wang et al. (2021) analysed the influence of processing parameters on the cutting front parameter for abrasive waterjet machining and reported as follows: the involved transverse speed was declared to have a substantial effect on the cutting front profile. However, the water pressure and abrasive flow rate were declared ineffective on the cutting front profile. The drawback of these articles is their inability to convert multiple responses into a single response, which promotes the concentration of efforts of the process engineer on specific parameters for enhanced process efficiency. Also, some of the methods are complicated and the process engineer may have difficulty applying them in practice.

Consequently, to avoid the restrictions of previous studies regarding complexity removal and the confusion of the process engineer in multiple-choice responses instead of dependence on the single response from enhanced efficiency, this study proposes two optimization approaches. The EDAS method is used as the foundation to enhance the efficiency of the abrasive waterjet machining process while processing the Ti-6Al-2Sn-4Zr-2Mo alloy while the DFA method converts the multiple responses into a single response to promote attention to the superior aspects of the AWJM process (Pradhan & Maity, 2018). As the authors are aware, this is the first time the two methods will be applied to solve the AWJM process optimization problem.

The EDAS method, originated by KeshavarzGhorabaee et al. in the year 2015 works efficiently where conflicting features prevail (Maduekwe & Oke, 2022). As a multicriteria tool, the EDAS method permits the ranking of experimental trials from experiments to choose the best rank which generates optimal parameters and the corresponding responses (Okponyia & Oke, 2021; Maduekwe & Oke, 2022). The desirability function analysis connotes the concept of the outstanding quality of a parameter in which this outlier is taken as exhibiting an overwhelming quality that others cannot beat. Therefore, the focus on quality improvement should be on the single chosen parameter.

In this article, the EDAS method and not other multicriteria approaches were deployed because as distinct from other multicriteria methods, the EDAS method disallows the subjective interest of people as inputs to the computations using questionnaires are not usually associated with the traditional EDAS method (Okponyia & Oke, 2021; Maduekwe & Oke, 2022). Furthermore, the DFA method was adopted as an optimization method in this work and not another optimization method such as the Taguchi method because it avoids the problem of not being able to distinguish superior parameters from another. Unlike the Taguchi method, when the ranks of the experimental trials are made, and the best experimental trial is identified, the indices produced to represent each parameter at the optimal points usually distinguish one parameter from the other regarding superiority.

2. METHODS

In this article, two methods, namely the EDAS method and the DFA method were independently employed as adequate approaches to achieve parametric optimization in machining planning for abrasive waterjet machining. While acknowledging the responsibility to change the raw Ti-6Al-2Sn-4Zr-2Mo alloy into parts usage by the jet engines, for instance, a chief focus of the process engineer is to optimize the machining

process. To implement the EDAS method, two measures, namely the desirability of options, broken down to the negative and positive distances from the average solution are needed (Okponyia & Oke, 2021; Maduekwe & Oke, 2022). The author of the EDAS method prides in the method's evasion of the concept of the ideal and nadir solutions for the principal parameters of the AWJM process (Okponyia & Oke, 2021; Maduekwe & Oke, 2022). For more details on the EDAS method, information is obtainable from Ulutas (2017).

2.1. Basis to Select Abrasive Waterjet Cutting Parameters

This section discusses the basis that guided the choice of the principal parameters for the abrasive waterjet cutting process analysed in this work. The abrasive waterjet machining process has the following principal equipment being maintained: accumulation water transmission lines, waterjet catchers, accumulators, hydraulic nuts, fluid additive process, intensifier, on/off valve, filter, waterjet nozzles, water transmission lines and abrasive waterjet nozzle (Johnston, 1989). If any of these equipment components fail, pressure will not be built up and the goal of the machine will not be achieved. Therefore, the waterjet pressure may be a leading parameter in the assessment of the AWJM process. Thus, the maintenance engineer strives to keep the AWJM process in a good form, building and discharging the desired pressure during operation. As pressurized water is delivered through the diamond-based nozzle to a mixing compartment, the pressure acts, developing a vacuum and attracting abrasive particles (sometimes garnet sand) to a pool directed at the Ti-6Al-2Sn-4Zr-2Mo alpha-beta alloy for cutting to take place.

Furthermore, the maintenance engineer that delivers a functional system to the process engineer is aware that building up the waterjet pressure for service is not enough; it must be delivered at the point of need. This necessitates the equipment design to allow the pressure movement to be a seemingly unnoticed back and forth as well as cross-over movement. This is the rate at which the pressure delivery equipment acts between cuts. Consequently, in an abrasive waterjet machining process, the traverse speed is important from the perspective of deploying an effective cutting strategy in the process. Besides, between the nozzles tip and the Ti-6Al-2Sn-4Zr-2Mo alpha-beta alloy, a distance should be maintained for effective delivery of pressure. Thus, to commence and complete the AWJM process, the standoff distance is a requirement for inclusion in the analysis. It is noted that as a high standoff distance is maintained between the nozzle and the material being processed, a higher spread of the abrasive jet is guaranteed. Consequently, the cross-sectional area targeted expands. In sum, this section has advocated the inclusion of waterjet pressure, standoff distance and traverse speed as important components of the AWJM process and hence suggested inclusion in the present study. In this study, based on the basis established for the parameters of the AWJM process, the experimental data of Perumal et al. (2020) was applied to validate the methods of EDAS and DFA used on the problem of parametric optimization of the AWJM process using Ti-6Al-2Sn-4Zr-2Mo alpha-beta alloy.

2.2. System Information

In the application of both the EDAS and DFA methods, the starting point in the analysis is to know the influence of the AWJM process parameters (factors) on the responses (outputs such as material removal rate and surface roughness). As such the specification of the parameters in an experiment is essential. Furthermore, these parameters are attached to a restricted number of possible values and these are generally known as factor levels. More specifically defined, a factor (parameter) in the AWJM process experiment represents an organized independent variable that the process engineer has set at diverse levels. Also, the levels of a factor may be described as the number of variations a parameter is subjected to during the AWJM process experiment. The schematic representation of the abrasive waterjet is shown in Figure 1 while Table 1 shows the factors (parameters) and their levels. Figure 1 shows the static positioning of the abrasive waterjet machine and the workpiece. However, in reality, cutting is accomplished while the tip of the nozzle moves in a programmed manner over the surface of the work material to be cut (Wang et al., 2021). The jet of high-pressure fluid from the machine makes the holes and the desired shapes as the jet pass over the surface of the material without touching it. It is the jet that comes into contact with the material and does the cutting process. In all cases, the materials are immersed in a water pool that cools them. If the holes are cut, water passes from the lower part of the container where the material is immersed with its lower part touching the water for cooling purposes.

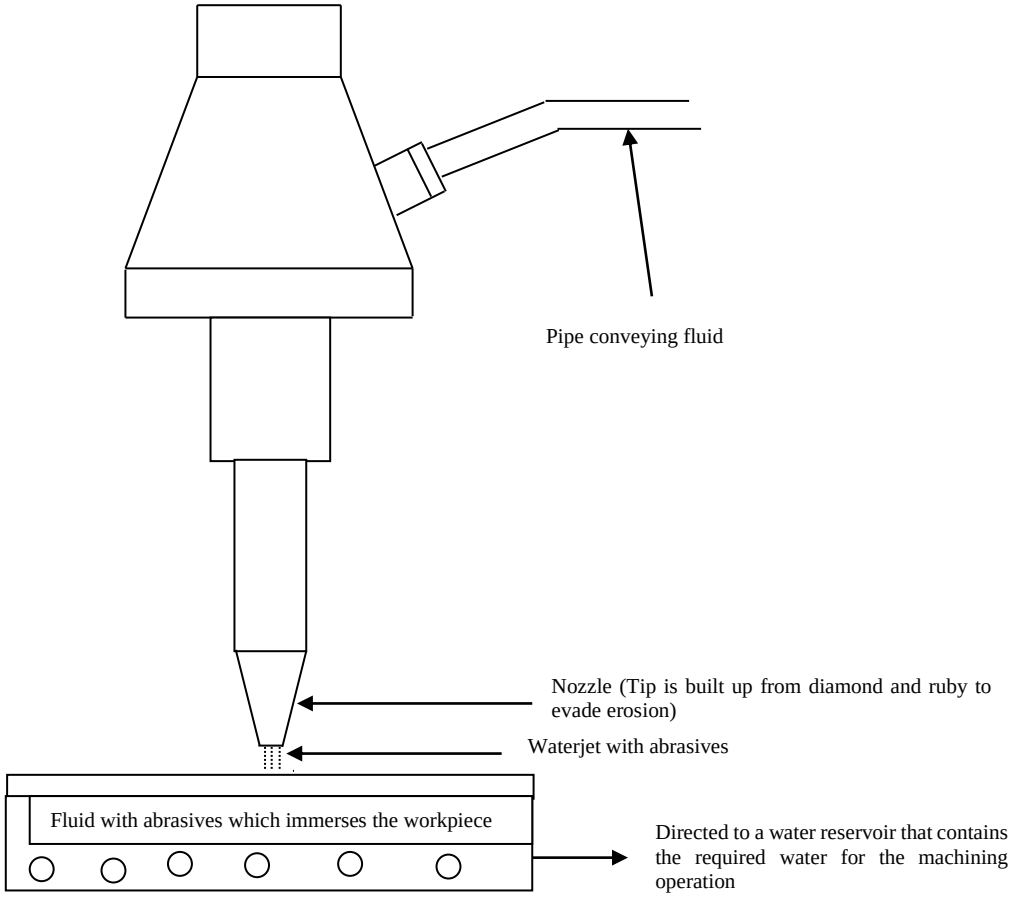

Figure 1. *Schematic of the abrasive waterjet*

The AWJM system consists of integrated parts that are well regulated including the hydraulic pump, hydraulic intensifier, drain and catcher system, accumulator, flow regulator valve, water reservoir, direction control valve, nozzle and mixing chamber or tube (Wang et al., 2021). The program control for the AWJM process is effective on the parts being manufactured. It is interesting to note that there are no tool changes (set up time) associated with the conventional CNC machine cutting system. As a result, substantial productivity of the system is guaranteed and the operator can produce more amounts of parts within the same time allocated to the conventional metal removal/cutting system. Furthermore, the program is flexible such that parts configuration changes could be made in a short period, thereby saving the enormous time lost to redrawing part configurations if the conventional CNC machine is to be used. Besides, the tailor-made program of the AWJM process allows the operator to cut shapes without previous knowledge of the CNC machine. Moreover, through the principle of particle erosion, the cutting of holes and part shapes are made in the AWJM process as opposed to the competing machining systems that work on frictional principles (i.e. friction drilling) and shearing. Thus, the abrasive waterjet machine produces superior outputs that avoid further finishing processes while eliminating additional machining activities such as reaming and boring and cost as well as ensuring that part integrity during service.

Table 1. *Factors and their levels (Perumal et al., 2020)*

Factor	Unit	Representation	Level 1	Level 2	Level 3
Water jet pressure	Bar	A	220	240	260
Traverse speed	mm/min	B	20	30	40
Standoff distance	Mm	C	1	2	3

Table 2 shows the orthogonal array, comprising columns that describe the test factors (parameters) and their associations. Usually, the format for defining an orthogonal array is to use the capital letter and follow it with a number that reveals the total number of an experiment to be conducted to arrive at the optimal parametric setting.

Table 2. *Cumulative data showing experimental results at all levels of the L27 orthogonal array method(Perumal et al., 2020)*

TrialNo	WJP (bar)	TS (mm/min)	SOD (mm)	MRR (mm^3/min)	Ra (μm)
1	220	20	1	81.3333	3.0006
2	220	20	2	84.1666	2.8713
3	220	20	3	86.8333	2.6366
4	220	30	1	116.5000	2.8620
5	220	30	2	119.2500	3.0583
6	220	30	3	121.2500	2.8153
7	220	40	1	151.6670	2.7560
8	220	40	2	153.3330	3.7006
9	220	40	3	160.2130	3.2143
10	240	20	1	78.3330	2.7311
11	240	20	2	82.5140	2.7893
12	240	20	3	85.5010	2.8156
13	240	30	1	116.1100	2.8030
14	240	30	2	121.2500	3.0353
15	240	30	3	125.2500	2.9540
16	240	40	1	150.2400	3.0516
17	240	40	2	159.0120	2.9406
18	240	40	3	163.3330	3.2403
19	260	20	1	80.1230	2.4000
20	260	20	2	84.4500	2.6930
21	260	20	3	87.3333	3.0670
22	260	30	1	115.7500	2.4681
23	260	30	2	119.500	2.9566
24	260	30	3	125.1200	3.3196
25	260	40	1	150.6670	3.0363
26	260	40	2	157.2040	3.1643
27	260	40	3	165.3330	3.5261

2.3. EDAS Method

The methodology used in obtaining EDAS is shown below (Okponyia & Oke, 2021; Maduekwe & Oke, 2022):

Step 1: Determine the average solutions (Okponyia & Oke, 2021; Maduekwe & Oke, 2022):

$$AV_j = \frac{\sum_{i=1}^{n} X_{ij}}{n} \tag{1}$$

where;

AV_j is the average of the respective output values

X_{ij} is the output values

n is the number of output values obtained

The average solution implies the sum of all the sets of the respective outputs of the AWJM process outputs divided by the number of values that are added. However, practically, it seems that the process engineer is spreading the value of the whole set equally between every number and walking back to observe what ends the value for the numbers. The idea of average is extremely useful for the AWJM process as it makes sense when analysing data from a large pool of material processing using the AWJM scheme.

Step 2: Calculate the Positive Distance from Average (PDA) and the Negative Distance from Average (NDA)

The EDAS method takes the average solution as the cornerstone of the computation for the method. The stage places the average number in the middle of the computation. It observes that there is the possibility of having deviations both to the right or left of the middle number (i.e. average). Suppose a number system is imagined and placed at the middle number, then the values to the left of the middle number are taken as the negative distance from the middle while numbers to the right of the middle (average) number are assumed to be positive distances from the average. Thus, each parameter of the AJWM process is taken each time with the value obtained at every experimental trial. If the value for the first trial is to the left, then all the values to the left are noted and applied to the formula. Also, if the values are to the right, showing a positive distance from the middle (average), they are accounted for in the analysis.

For the PDA

When the output is to be maximized (Okponyia & Oke, 2021; Maduekwe & Oke, 2022):

$$PDA_{ij} = \frac{\max(0,(X_{ij} - AV_j)}{AV_j} \tag{2}$$

Equation (2) is used in the EDAS method to compute the positive distance from the average solutions. To apply Equation (2), the researcher counts only the positive numbers within the range of values considered. Then the sum of only the positive numbers is made. To maximize, the higher value of zero and the difference between the output value and the average of the respective output value is made. The obtained value is then divided by the average of the respective output values.

When the output is to be minimized (Okponyia & Oke, 2021; Maduekwe & Oke, 2022):

$$PDA_{ij} = \frac{\max(0,(AV_j - X_{ij})}{AV_j} \tag{3}$$

Equation (3) is also used in the EDAS method to compute the positive distance from the average solutions but for the minimization case. To minimize, the higher value of zero and the difference between the average of the respective output values and the output value is obtained. The outcome is then divided by the average of the respective output values.

For the NDA

When the output is to be maximized (Okponyia & Oke, 2021; Maduekwe & Oke, 2022):

$$NDA_{ij} = \frac{\max(0,(AV_j - X_{ij})}{AV_j} \tag{4}$$

Equation (4) shows the negative distance from the average solutions where the output is maximized. Here, the higher value between zero and the difference between the average of the respective output values and the output value is calculated. Then the emerging result is divided by the average of the respective output values.

When the output is to be minimized (Okponyia & Oke, 2021; Maduekwe & Oke, 2022):

$$NDA_{ij} = \frac{\max(0,(X_{ij} - AV_j)}{AV_j} \tag{5}$$

Equation (5) reveals the negative distance from the average solutions for a situation where the output is minimized. Here, the greater value between zero and the difference occurring between the output value of interest and the average of the various outputs is obtained.

Step 3: Obtain the Weighted sum of PDA and NDA

This is obtained by multiplying the PDA and NDA values by the weightage of the output.

Step 4: Obtain the SPi (Sum of weighted PDA values) and SNi (Sum of weighted NDA values) (Okponyia & Oke, 2021; Maduekwe & Oke, 2022):

$$SP_i = \sum_{j=1}^{m} PDA_{ij} \tag{6}$$

Equation (6) is the weighted sum of the positive distance from the average solutions. This is a method of analysis when conducting a sum of the AWJM process data to give some of the parameters more weights such that they exhibit greater influence on the results than other parameters. In this situation of weighing, the product of the response variable associated with specific parameters and the weight variable is found to obtain either the weighted sum of the negative distance from the average solution, Equation (6) or the weighted sum of the positive distance from the average solution Equation (7). Nonetheless, the number of observations considered for the response variable should be equal to that contemplated for the weights variable (Okponyia & Oke, 2021; Maduekwe & Oke, 2022).

$$SN_i = \sum_{j=1}^{m} w_j NDA_{ij} \tag{7}$$

Step 5: Normalize the values of SP and SN (Okponyia & Oke, 2021; Maduekwe & Oke, 2022):

$$NSP_i = \frac{SP_i}{\max_i(SP_i)} \tag{8}$$

Equation (8) shows the normalization formula for the sum of the weighted positive distance from the average solutions. It means that for the AWJM process data, the values evaluated are attuned from various magnitudes to a common magnitude such that a comparison of the strength of each experimental trial outcome from another could be judged. Besides, the added advantages of normalizing include the opportunity to eliminate redundant AWJM process data through observation. It also promotes the organization of the AWJM process database. Furthermore, the process engineer has the opportunity to logically group data. By considering Equation (8), the normalized values for the sum of the weighted positive distance from the average solution are obtained considering each S.Pi and concurrently dividing it by the maximum value available for all the SPi. Equation (9) is obtained by first obtaining the ratio of the sum of weighted negative distances from the average solutions to the possible maximum values from all the SNi. This outcome is then subtracted from 1 (Okponyia & Oke, 2021; Maduekwe & Oke, 2022).

$$NSN_i = 1 - \frac{SN_i}{\max_i(SN_i)} \tag{9}$$

Step 6: Normalize the values of NSP and NSN (Okponyia & Oke, 2021; Maduekwe & Oke, 2022):

$$AS_i = \frac{1}{2}(NSP_i + NSN_i) \tag{10}$$

Further normalization of the values obtained from the previous step is pursued such that AS_i, defined as the averages of the values obtained from Equations (8) and (9) is obtained and termed Equation (10). The values of $AS_i$are ranked from largest to smallest values and the top ranking.

2.4. DFA method

The objective of the DFA is to find the optimal parametric setting that gives the best compromise considering two objectives:

1. Maximal Material Removal Rate (MRR)
2. Minimal Surface Roughness) (Ra)

Steps involved in implementing DFA (Pradhan & Maity, 2018):

1. Calculate the desirability index
2. Compute the composite desirability: Combining the individual desirability index of all responses to a single value
3. Determining the optimum level and its combination

to minimize Surface Roughness, The formula below is used to obtain the desirability index for the Surface Roughness

$$d_i = \begin{cases} 1, y_j \le y_{min} \\ \left(\dfrac{y_j - y_{max}}{y_{min} - y_{max}}\right)^r, y_{min} \le y_j \le y_{max}, r \ge 0 \\ 0, y_j \ge y_{min} \end{cases} \tag{11}$$

where

d_i is the desirability index

y_j is the current output value

y_{max} is the maximum output value

y_{min} is the minimum output value

r is the shape constant

Equation (11) is an index that allocates a score to three response categories (Pradhan & Maity, 2018). In the first category, a score of 1 is assigned when y, is not greater than ymin. However, the second category is to assign a score of zero when y; is not less than ymin. But the third category of score assignment is done when it is observed that the yj is calculated which fall between ymin and ymax. Then a score is calculated based on the rth power of the ratio between the difference of ymax from yj and the difference of ymax from ymin. In this case, all the values of r used should be positive. This description (Equation (11)) fits the surface roughness evaluation using the desirability function analysis since the mini values of surface roughness are beneficial to the process and therefore accommodated in the formula. The shape constant of 2 is adopted in this case. Furthermore, Equation (12) is used to obtain the desirability index for the material removal rate since it is to be maximized (Pradhan & Maity, 2018).

$$d_i = \begin{cases} 0, y_j \le y_{min} \\ \left(\dfrac{y_j - y_{max}}{y_{min} - y_{max}}\right)^r, y_{min} \le y_j \le y_{max}, r \ge 0 \\ 1, y_j \ge y_{min} \end{cases} \quad (12)$$

where

d_i is the desirability index

y_j is the current output value

y_{max} is the maximum output value

y_{min} is the minimum output value

r is the shape constant

However, when considering the material removal rate, the reverse is the case, Equation (12). Here, an index is formed which allocates scores to three different categories. For the first category, a score of zero is allocated when yj is not greater than ymin. Nonetheless, for the second group, a score of 1 is made as to the y; is not less than ymin. Moreover, for the third group, score assignment is conducted when it is observed that the yj being computed falls between ymax and ymin. Then a score is computed depending on the rth power of the ratio between the difference of ymin from yj and the difference of ymin from ymax. In this case, all these values of r used should be positive. This description stands for Equation (12).

$$d_c = \sqrt[w]{(d_1 \times d_2 \times .. d_i)} \quad (13)$$

Where

d_c is the composite desirability

w is the number of responses

d_i is the individual desirability

Furthermore, Equation (13) is obtained as the composite desirability factor (Pradhan & Maity, 2018). This is achieved by first recognizing the number of responses available in the AWJM process optimization problem. Then, the individual desirability is computed. To obtain the composite desirability, dc, each of the individual desirability is multiplied by one another and the wth root of the product obtained.

3. RESULTS AND DISCUSSION

This study into the optimization of process parameters of the AWJM process was conducted through an experiment involving three factors, namely, waterjet pressure, traverse speed and standoff distance. The level component of the factor-level framework has three levels, namely 1, 2 and 3. The AWJM process involved

the machining of the Ti-6Al-2Sn-4Zr-2Mo alpha-beta alloy, targeting the maximization of the material removal rate and the minimization of the surface roughness of the processed material. From the experiment, the results of the application of EDAS are shown after using Table 3 as an input, in Table 4. Afterwards, the final results are shown accordingly and then the results for the DFA method are displayed. For the EDAS method, by implementing Equations (1) to (10), the values of the ASi, which were ranked are revealed. The DFA method shows a two-stage process where the desirability index is obtained with ranks of the experimental trials to reveal the superiority of an experimental trial over the other. Then, this provides a point where the optimal values for all the parameters, including the waterjet pressure, standoff distance and traverse speed are indicated together with the responses, which are the material removal rate and surface roughness.

3.1 Implementing EDAS

Step 1: Determine the average solutions

To obtain Table 3, Equation (1) is applied. Here, the computation of the AVj is conducted by considering the values of each of the responses (material removal rate and surface roughness) and obtaining the averages.

Table 3. *Obtaining average solutions for the material removal rate and the surface roughness*

S. No	WJP (bar)	TS (mm/min)	SOD (mm)	MRR (mm3/min)	Ra (μm)	S. No	WJP (bar)	TS (mm/min)	SOD (mm)	MRR (mm3/min)	Ra (μm)
1	220	20	1	81.3333	3.0006	15	240	30	3	125.2500	2.9540
2	220	20	2	84.1666	2.8713	16	240	40	1	150.2400	3.0516
3	220	20	3	86.8333	2.6366	17	240	40	2	159.0120	2.9406
4	220	30	1	116.5000	2.8620	18	240	40	3	163.3330	3.2403
5	220	30	2	119.2500	3.0583	19	260	20	1	80.1230	2.4000
6	220	30	3	121.2500	2.8153	20	260	20	2	84.4500	2.6930
7	220	40	1	151.6670	2.7560	21	260	20	3	87.3333	3.0670
8	220	40	2	153.3330	3.7006	22	260	30	1	115.7500	2.4681
9	220	40	3	160.2130	3.2143	23	260	30	2	119.5000	2.9566
10	240	20	1	78.3330	2.7311	24	260	30	3	125.1200	3.3196
11	240	20	2	82.5140	2.7893	25	260	40	1	150.6670	3.0363
12	240	20	3	85.5010	2.8156	26	260	40	2	157.2040	3.1643
13	240	30	1	116.1100	2.8030	27	260	40	3	165.3330	3.5261
14	240	30	2	121.2500	3.0353					Average	120.0581	2.9595
										Weightage	0.5	0.5

By starting with the material removal rate, the value of experimental trial 1 is 81.3333mm3/min. This is added to the next for experimental trial 2, which is 84.1666mm3/min to yield a cumulative value of 165.4999mm3/min. further cumulative additions and done on each other experimental trials 3, to 27 to obtain a total value of 3241.57mm3/min. when divided by the total number of observations, 27, the average value is 120.0581mm3/min. The same procedure is adopted for the computation of the roughness average, Ra, for surface roughness, which also has 27 experimental trials. In this case, the total value is 79.9068mm while the average is obtained as 79/9068mm. However, for further calculations, an equal weight of importance of the outputs is assumed it was not stated that the material removal rate is more important than surface roughness or the reverse. Hence, a 50:50 (i.e. 0.5 for material removal rate and 0.5 for roughness average) weight of outputs is given.

Step 2: Calculate the Positive Distance from Average (PDA) and the Negative Distance from Average (NDA)

Step 3: This is obtained by multiplying the PDA and NDA values by the weightage of the output.

Table 4. *Positive Distance from Average (PDA) and Negative Distance from Average (NDA)*

	Positive Distance from Average				Negative Distance from Average			
S.No.	MRR	MRR (weighted)	Ra	Ra (weighted)	MRR	MRR (weighted)	Ra	Ra (weighted)
1	0.0000	0.00000	0.0000	0.0000	0.3226	0.1613	0.0139	0.0069
2	0.0000	0.00000	0.0298	0.0149	0.2990	0.1495	0.0000	0.0000
3	0.0000	0.00000	0.1091	0.0546	0.2767	0.1384	0.0000	0.0000
4	0.0000	0.00000	0.0329	0.0165	0.0296	0.0148	0.0000	0.0000
5	0.0000	0.00000	0.0000	0.0000	0.0067	0.0034	0.0334	0.0167
6	0.0099	0.00496	0.0487	0.0244	0.0000	0.0000	0.0000	0.0000
7	0.2633	0.13164	0.0688	0.0344	0.0000	0.0000	0.0000	0.0000
8	0.2772	0.13858	0.0000	0.0000	0.0000	0.0000	0.2504	0.1252
9	0.3345	0.16723	0.0000	0.0000	0.0000	0.0000	0.0861	0.0430
10	0.0000	0.00000	0.0772	0.0386	0.3475	0.1738	0.0000	0.0000
11	0.0000	0.00000	0.0575	0.0288	0.3127	0.1564	0.0000	0.0000
12	0.0000	0.00000	0.0486	0.0243	0.2878	0.1439	0.0000	0.0000
13	0.0000	0.00000	0.0529	0.0264	0.0329	0.0164	0.0000	0.0000
14	0.0099	0.00496	0.0000	0.0000	0.0000	0.0000	0.0256	0.0128
15	0.0432	0.02162	0.0019	0.0009	0.0000	0.0000	0.0000	0.0000
16	0.2514	0.12570	0.0000	0.0000	0.0000	0.0000	0.0311	0.0156
17	0.3245	0.16223	0.0064	0.0032	0.0000	0.0000	0.0000	0.0000
18	0.3604	0.18022	0.0000	0.0000	0.0000	0.0000	0.0949	0.0474
19	0.0000	0.00000	0.1891	0.0945	0.3326	0.1663	0.0000	0.0000
20	0.0000	0.00000	0.0901	0.0450	0.2966	0.1483	0.0000	0.0000
21	0.0000	0.00000	0.0000	0.0000	0.2726	0.1363	0.0363	0.0182
22	0.0000	0.00000	0.1660	0.0830	0.0359	0.0179	0.0000	0.0000
23	0.0000	0.00000	0.0010	0.0005	0.0046	0.0023	0.0000	0.0000
24	0.0422	0.02108	0.0000	0.0000	0.0000	0.0000	0.1217	0.0608
25	0.2550	0.12748	0.0000	0.0000	0.0000	0.0000	0.0260	0.0130
26	0.3094	0.15470	0.0000	0.0000	0.0000	0.0000	0.0692	0.0346
27	0.3771	0.18855	0.0000	0.0000	0.0000	0.0000	0.1914	0.0957

The first segment of Table 4, which is the second to the fifth column, is computed from Equations (2) and (3) where the positive distance from the average solutions is considered with output to be maximized from Equation (2). This is relevant for the material removal rate because it is beneficial for the AWJM process to increase the rate of material removal in the system and attain utmost efficiency and power savings (energy cost reduction) since the elongated time of material removal gives the additional cost to the AWJM process. Consider experimental trial 1 in the first segment of Table 4, by applying Equation (2) for the material removal rate component of the table, the researchers seek to evaluate Equation (2) by first considering the numerator and then dividing the outcome by the denominator. The numerator instructs the researchers to obtain the maximum value between zero and the other component of the numerator. This other component, containing Xij and AVj represent 81.3333mm3/min (for X11) and 120.0581mm3/min (for AVj), respectively (Table 3). This yields 81.3333mm3/min-120.0581mm3/min (i.e. -38.72mm3/min). Then the maximum of zero and -38.7248 mm3/min is obtained as zero. By dividing this outcome, zero by the denominator, i.e. 120.0581mm3/min, a value of zero is finally obtained as displayed in the second column and experimental trial 1 in the first segment of Table 4. However, recall that a weight of 0.5 was achieved for the material removal rate. This, if multiplied by the outcome of the MRR (i.e. 0), as 0 x 0.5, a weighted MRR of 0 is obtained. As the same procedure is adopted for experimental trials 2 to 27, the results for columns two and three for Table 4 are obtained. Also, note that the same procedure is obtainable for the computation of the roughness average and the fourth and fifth columns of Table 4 are obtained. Hence, by calculating for all the experimental trials 1 to 27, all the columns for the MRR and Ra are completed with values of weighted MRR and weighted Ra accounted for.

The second segment of Table 4, which is the sixth to the nineth column is obtained from Equations (4) and (5) where the negative distance from the average solutions considered and the output is to be maximized (i.e. material removal rate) is for Equation (4). In Equation (5), the output is to be minimized (i.e. surface roughness measured by the roughness average, Ra in Table 4. By applying Equation (4) to the material removal rate component of the table, the researchers seek to appraise Equation (4) by first considering the numerator and then dividing the outcome by the denominator. The numerator reveals to the researchers that to obtain it, there should be a consideration of the maximum value between zero and the difference between the AV, and Xij. By starting with the experimental trial 1 in the second seegment of Table 4, Table 3 is referred to first to extract the values of AVj and X11, for the MRR since the maximization of output is sought. The value of AVj - X11 is 120.0581mm3/min - 81.3333mm3/min and this gives 38.7248mm3/min. Then the maximum of 38.7248mm3/min and zero is given as 38.7248mm3/min. This value is divided by AVj (i.e. 120.0581mm3/min) to yield 03226mm3/min. When multiplied by the weight of 0.5, a weighted MRR value of 0.1613mm3/min is obtained. These values are shown for MRR and weighted MRR for experimental trial 1 in columns 6 and 7 of the second row of Table 4. By following a similar procedure, all the experimental trials 2 to 27 may be evaluated. Also, Equation (5) could be applied likewise for the NDAij where the surface roughness minimization is of interest and the second segment of Table 4 will be completed.

Step 4: Obtain the SPi (Sum of weighted PDA values) and SNi (Sum of weighted NDA values)

Here, Equations (6) and (7) are applied to produce Table 5.

Table 5. *The Sum of weighted PDA and NDA values*

	Sum of weighted PDA values			Sum of weighted NDA values		
S.No.	Weighted MRR	Weighted RA	SPi	Weighted MRR	Weighted RA	SPi
1	0.0000	0.0000	0.0000	0.1613	0.0069	0.1682
2	0.0000	0.0149	0.0149	0.1495	0.0000	0.1495
3	0.0000	0.0546	0.0546	0.1384	0.0000	0.1384
4	0.0000	0.0165	0.0165	0.0148	0.0000	0.0148
5	0.0000	0.0000	0.0000	0.0034	0.0167	0.0201
6	0.0050	0.0244	0.0293	0.0000	0.0000	0.0000
7	0.1316	0.0344	0.1660	0.0000	0.0000	0.0000
8	0.1386	0.0000	0.1386	0.0000	0.1252	0.1252
9	0.1672	0.0000	0.1672	0.0000	0.0430	0.0430
10	0.0000	0.0386	0.0386	0.1738	0.0000	0.1738
11	0.0000	0.0286	0.0288	0.1564	0.0000	0.1564
12	0.0000	0.0243	0.0243	0.1439	0.0000	0.1439
13	0.0000	0.0264	0.0264	0.0164	0.0000	0.0164
14	0.0050	0.0000	0.0050	0.0000	0.0128	0.0128
15	0.0216	0.0009	0.0226	0.0000	0.0000	0.0000
16	0.1257	0.0000	0.1257	0.0000	0.0156	0.0156
17	0.1622	0.0032	0.1654	0.0000	0.0000	0.0000
18	0.1802	0.0000	0.1802	0.0000	0.0474	0.0474
19	0.0000	0.0945	0.0945	0.1663	0.0000	0.1663
20	0.0000	0.0450	0.0450	0.1483	0.0000	0.1483
21	0.0000	0.0000	0.0000	0.1363	0.0182	0.1544
22	0.0000	0.0830	0.0830	0.0179	0.0000	0.0179
23	0.0000	0.0005	0.0005	0.0023	0.0000	0.0023
24	0.0211	0.0000	0.0211	0.0000	0.0608	0.0608
25	0.1275	0.0000	0.1275	0.0000	0.0130	0.0130
26	0.1547	0.0000	0.1547	0.0000	0.0346	0.0346
27	0.1886	0.0000	0.1886	0.0000	0.0957	0.0957

Note the Max SPi is 0.1886 while Max SNi is 0.1738.

Step 5: Normalize the values of SP and SN

Equations (8) and (9) are applied to the data to produce Table 6.

Table 6. *Normalised values of SP and SN (positive), Normalised values of SP and SN (negative) and Ranking of ASi values*

	Normalised Values of SP and SN (positive)		Normalised Values of SP and SN (negative)		Ranking of ASi values	
S.No.	SPi	NSPi	Sni	NSni	ASi	Rank
1	0.0000	0.0000	0.1682	0.0320	0.0160	27
2	0.0149	0.0790	0.1495	0.1398	0.1094	24
3	0.0546	0.2893	0.1384	0.2037	0.2465	20
4	0.0165	0.0874	0.0148	0.9147	0.5010	14
5	0.0000	0.0000	0.0201	0.8846	0.4423	17
6	0.0293	0.1555	0.0000	1.0000	0.5778	10
7	0.1660	0.8805	0.0000	1.0000	0.9403	1
8	0.1386	0.7350	0.1252	0.2795	0.5072	13
9	0.1672	0.8869	0.0430	0.7523	0.8196	4
10	0.0386	0.2047	0.1738	0.0000	0.1023	25
11	0.0288	0.1525	0.1564	0.1002	0.1264	23
12	0.0243	0.1289	0.1439	0.1718	0.1504	22
13	0.0264	0.1402	0.0164	0.9054	0.5228	12
14	0.0050	0.0263	0.0128	0.9263	0.4763	16
15	0.0226	0.1196	0.0000	1.0000	0.5598	11
16	0.1257	0.6666	0.0156	0.9105	0.7886	7
17	0.1654	0.8773	0.0000	1.0000	0.9387	2
18	0.1802	0.9558	0.0474	0.7270	0.8414	3
19	0.0945	0.5013	0.1663	0.0429	0.2721	19
20	0.0450	0.2388	0.1483	0.1466	0.1927	21
21	0.0000	0.0000	0.1544	0.1112	0.0556	26
22	0.0830	0.4403	0.0179	0.8968	0.6685	9
23	0.0005	0.0026	0.0023	0.9866	0.4946	15
24	0.0211	0.1118	0.0608	0.6499	0.3809	18
25	0.1275	0.6761	0.0130	0.9253	0.8007	6
26	0.1547	0.8205	0.0346	0.8009	0.8107	5
27	0.1886	1.0000	0.0958	0.4491	0.7246	8
			0.1738			

Step 6: Normalize the values of NSP and NSN

Equation (10) is applied to the data to obtain Table 6. The values of ASi are ranked from largest to smallest values and the top ranking. The optimal parametric setting is given to be located at number 7, and the input and output parameters at number 7 of the orthogonal array. It holds the optimal result where MRR is sought to be maximized and Ra is sought to be minimized. The optimal results are waterjet pressure of 220bar, traverse speed of 40mm/min, and stand-off distance of 1mm. However, the output is an MRR of 151.667mm3/min, and a roughness average, Ra, of 2.756mm.

To implement the desirability function, a two-stage process is followed. First, the desirability index and composite desirability is then formed. Table 7 shows the experimental values of the surface roughness response and the material removal rate and the corresponding desirability indices. To obtain Table 7, the following explanations prevail. Consider the second column and the first row which indicate the surface roughness value of 3.0006mm, extracted from the experimental data by Perumal et al. (2020). However, it is

known that surface roughness in the AWJM process is to be minimized. Then, Equation (11) is used to optimize the surface roughness. From the data are given in Perumal et al. (2020), the data for yj, ymin and ymax are obtainable as yj (=y1 for experimental trial 1), ymin is 2.4000mm and ymax is 3. 706mm. Notice that the analysis relates to experimental trial 1 and the corresponding surface roughness value is 3.0006mm, which is the entry in the last column of Table 2 for experimental trial 1. Also, the ymax value is read from the last column of experimental trial 8, which is the last column of Table 2. Also, the ymin is obtainable at experimental trial 19. Now, in applying Equation (11), the first option is to assign a value of 1 of yj ≤ ymin. But yj(=y1) = 3.0006mm is not less but greater than ymin at a value of 2.4000mm. Therefore, the first option of yj ≤ ymin is not respected. Then, the second option where the condition of assigning zero where yj ≥ ymax is considered. Here, y1, which is 3.0006mm is not greater than ymax value of 3.706mm. Therefore, the second condition is violated. However, it is the third condition where the rth power of the ratio of the difference between yj and ymax to the difference between ymin and ymax is considered. In this case, considering the numerator of the factor, yj–ymax, the difference is 0.6006mm. Also considering the denominator, ymin-ymax yields -0.3006mm since ymin is 2.400mm and ymax is 3.7006mm. The ratio of these two items yields -0.3. But this outcome of -0.3 is raised to be the power of 2, which makes the solution to be 0.09. This is used for further processing in the data analysis.

Table 7. *Experimental values of surface roughness and the material removal rate values with their desirability index*

S.No.	SR	SR-DI	MRR	MRR-DI	S.No.	SR	SR-DI	MRR	MRR-DI
1	3.0006	0.2897	81.3333	0.0012	15	2.9540	0.3296	125.2500	0.2908
2	2.8713	0.4066	84.1666	0.00450	16	3.0516	0.2490	150.2400	0.6831
3	2.6366	0.6693	86.8333	0.0095	17	2.9406	0.3415	159.0120	0.8600
4	2.8620	0.4157	116.5000	0.1925	18	3.2403	0.1253	163.3330	0.9546
5	3.0583	0.2439	119.2500	0.2212	19	2.4000	1.0000	80.1230	0.0004
6	2.8153	0.4633	121.2500	0.2433	20	2.6930	0.6002	84.4500	0.0049
7	2.7560	0.5275	151.6670	0.7105	21	3.0670	0.2373	87.3333	0.0107
8	3.7006	0.0000	153.3330	0.7432	22	2.4681	0.8980	115.7500	0.1850
9	3.2143	0.1398	160.2130	0.8858	23	2.9566	0.3272	119.5000	0.2239
10	2.7311	0.5557	78.3330	0.0000	24	3.3196	0.0858	125.1200	0.2892
11	2.7893	0.4909	82.5140	0.0023	25	3.0363	0.2609	150.6670	0.6913
12	2.8156	0.4630	85.5010	0.0068	26	3.1643	0.1700	157.2040	0.8219
13	2.8030	0.4763	116.1100	0.1885	27	3.5261	0.0180	165.3330	1.0000
14	3.0353	0.2617	121.2500	0.2433					

Step 2 - Compute the composite desirability

The aim of arriving at the composite desirability is to reduce the multi-repose objective function to a single response objective function. It is achieved by implementing a composite desirability equation to obtain the desirability by considering all the outputs and finding a compromise. Equation (13) is used to obtain the desirability (Figure 2).

The rank computations reveal the 1st, 2nd and 3rd positions to experimental trials 7 (MRR-DI, 0.7105; RA-DI, 0.5275; Comp_Des, 0.6122), 17 (MRR-DI, 0.8600; RA-DI, 0.3415; Comp_Des, 0.5419) and 25 (MRR-DI, 0.6913; RA-DI, 0.2609; Comp_Des, 0.4247), respectively.

In Perumal et al. (2020), the authors concluded by declaring the obtained optimal results as waterjet pressure of 260 bar, traverse speed of 40mm/min and standoff distance of 1mm. Compared to the results obtained by EDAS and DFA methods, particularly experimental trial 7 in Table 6 and validated by experimental trial 7 of Figure 2, where the instances are for the EDAS and DFA methods, respectively, our results are better as it requires less energy for its implementation in the AWJM process. The obtained results are waterjet pressure of 220bar, traverse speed of 40mm/min, and stand-off distance of 1mm. However, the output is an MRR of 151.667mm3/min, and a roughness average, Ra, of 2.756mm.

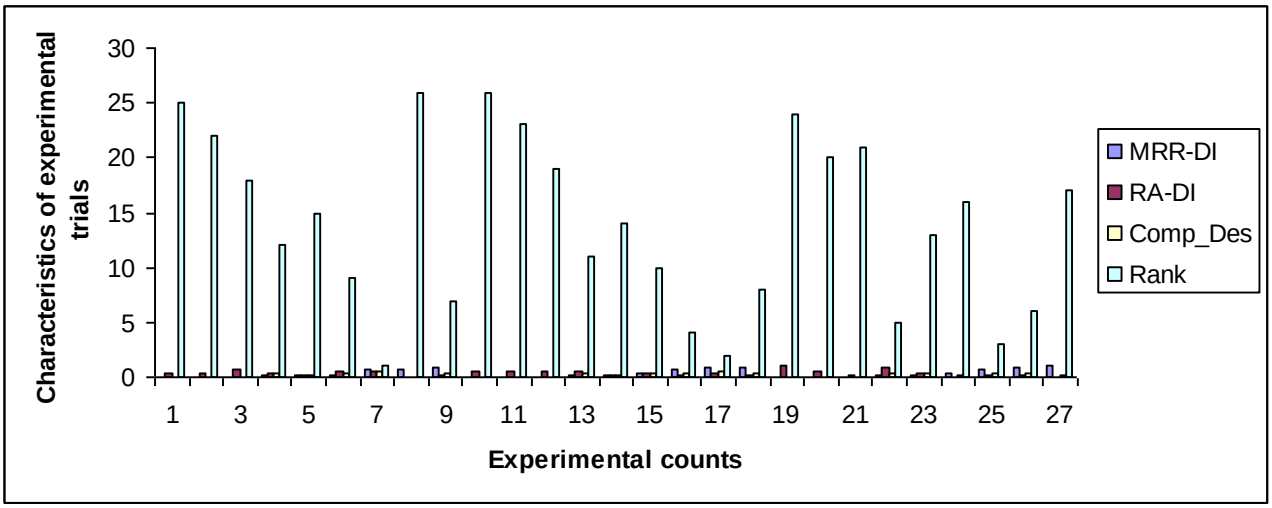

Figure 2. *Desirability ındex of material removal rate and surface roughness with the composite desirability and the ranks according to the desirability of the parametric settings.*
MRR-DI*: desirability index of material removal rate;*
RA-DI*: desirability index of surface roughness (roughness average);*
Comp_Des*: composite desirability)*

Furthermore, from the results of the case examining the abrasive waterjet machining using the Ti-6Al-2Sn-4Zr-2Mo alpha-beta alloy, it seems that both the EDAS method and the DFA method are suitable tools to articulate the optimization characteristics of the AWJM process. Undeniably, the EDAS method is capable to confine and handle parametric information and helping the decision-maker to decide on what threshold of input resources to use for the AWJM process. Consider the three parameters of waterjet pressure, traverse speed and standoff distance labelled as critical parameters in Perumal et al. (2020) whose data is used to validate the procedures of EDAS and DFA. The closest parameter to the operations in the abrasive waterjet orifice is perhaps the waterjet pressure. In this situation, the operator has two options to simulate the results of the waterjet pressure and the corresponding outcomes in material removal rate and surface roughness. The first option entails the operator mixing the granite particles with water within the mode boundaries while the mixed substance is passed through the orifice (Singh et al., 2021). A second option is to add the granite to water before passing it to the nozzle and afterwards, the AWJM is applied to cut the Ti-6Al-2Sn-4Zr-2Mo alpha-beta alloy. This is an action and other actions may include the operations of several other units of the abrasive waterjet machining process such as the accumulation water transmission lines, waterjet catchers, accumulators, hydraulic unit, fluid additive process, intensifier, on/off value, filters, waterjet nozzles, water transmission lines and abrasive water jet nozzle (Johnston, 1989). Thus, all the above actions could be made flexible such that the sensitivity of the parameters could be estimated. This means that the EDAS method allows the process engineer to explain the influence of changes in parametric values of one or more parameters in individual or combined states on the outcomes (material removal rate and surface roughness). Furthermore, the process engineer is satisfied with the adaptability of the DFA method when developing possible outcomes with varying levels of inputs. The clarity and simplicity of the EDAS and DFA methods are important advantages that support the transmission of information between the operator and the process engineer in the AWJM process, leading to more accurate and reliable results for decision-making. Besides, both the EDAS and DFA methods may be deployed for synergy with other methods such as Taguchi and data envelopment analysis which is crucial when developing action plans from performance outcomes.

4. CONCLUSIONS

The study sheds light on the optimal parametric determination of the Ti-6Al-2Sn-4Zr-2Mo alloy processed through abrasive waterjet machining and provides recommendations when two robust methods of EDAS and DFA were applied. The applications of the two methods led to the following conclusions. The applications of both the EDAS and DFA methods as multicriteria abrasive waterjet cutting decision-making tools to solve

the new problem of process parametric optimization using the Ti-6Al-2Sn-4Zr-2Mo alpha-beta material is feasible. In the process of the Ti-6Al-2Sn-4Zr-2Mo alloy for high temperature and loading applications, there is a need to focus on a waterjet of 220bar, traverse speed of 40mm/min and standoff distance of 1mm. the accompanying metal removal rate is 151.667mm3/min and the roughness average of 2.76mm. These results apply to both methods as the DFA method validated the results of the EDAS method. More prospective studies could develop methods that integrate the EDAS and DFA methods where one method overcomes the drawbacks of the other. Apart, additional studies may consider the sensitivity analysis of the parameters based on each method.

CONFLICT OF INTEREST

The authors declare no conflict of interest.

REFERENCES

Akkurt, A. (2004). Waterjet cutting systems and assesment of their industrial applications. *Journal of Polytechnic*, *7*(2), 129-139

Bhamare, S., Ramakrishnan, G., Mannava, S. R., Langer, K., Vasudevan, V. K., & Qian, D. (2013). Simulation-based optimization of laser shock peening process for improved bending fatigue life of Ti–6Al–2Sn–4Zr–2Mo alloy. *Surface and Coatings Technology*, *232*, 464-474. doi:10.1016/j.surfcoat.2013.06.003

Chen, M., Zhang, S., Zeng, J., Chen, B., Xue, J., & Ji, L. (2019). Correcting shape error on external corners caused by the cut-in/cut-out process in abrasive water jet cutting. *The International Journal of Advanced Manufacturing Technology*, *103*, 849-859. doi:10.1007/s00170-019-03564-x

Ergür, H. S. (2009). Theoretical analysis of abrasive waterjet and modelling with artificial neural network. *Journal of Engineering and Architecture Faculty of Eskişehir Osmangazi University*, *22*(2), 179-197

Fleißner-Rieger, C., Pfeifer, T., Turk, C., & Clemens, H. (2022) Optimization of the post-process heat treatment strategy for a near-α titanium base alloy produced by laser powder bed fusion. *Materials*, *15*(3), 1032. doi:10.3390/ma15031032

Hashish, M. (2014). Waterjet Machining Process. In: A. Nee (Eds.), *Handbook of Manufacturing Engineering and Technology* (pp. 1-30). Springer. doi:10.1007/978-1-4471-4976-7_75-1

Iqbal, A., Dar, N. U., & Hussain, G. O. (2011). Optimization of abrasive water jet cutting of ductile materials. *Journal of Wuhan University of Technology - Materals Science Edition*, *26*, 88-92. doi:10.1007/s11595-011-0174-8

Johnston, C. E. (1989). Waterjet/Abrasive Waterjet Machining. In: *ASM Handbook, 16, Machining* (pp. 520-527). ASM International. doi:10.31399/asm.hb.v16.a0002158

Karakurt, İ., Aydın, G., Yıldırım, F., & Kaya, S. (2019, April 16-19). *Current technological developments in cutting applications by abrasive waterjet*. In: 26th International Mining Congress and Exhibition of Turkey (pp. 1334-1339).

Kartal, F. (2017). A review of the current state of abrasive water-jet turning machining method. *International Journal of Advanced Manufacturing Technology*, *88*, 495-505. doi:10.1007/s00170-016-8777-z

Maduekwe, V. C., & Oke, S. A. (2022). The application of the EDAS method in the parametric selection scheme for maintenance plan in the Nigerian food industry. *Journal Rekayasa Sistem Industri*, *11*(1), 1-22. doi:10.26593/jrsi.v11i1.4349.1-22

Marya, M., & Edwards, G. R. (2002). An analytical model for the optimization of the laser bending of titanium Ti–6Al–2Sn–4Zr–2Mo.*Journal of Materials Processing Technology*, *124*(3), 337-344. doi:10.1016/S0924-0136(02)00223-6

Miao, X., Qiang, Z., Wu, M., Song, L., & Ye, F. (2018). The optimal cutting times of multipass abrasive water jet cutting. *The International Journal of Advanced Manufacturing Technology*, *97*, 1779-1786. doi:10.1007/s00170-018-2011-0

Muthuramalingam, T., Vasanth, S., Vinothkumar, P., Geethapriyan, T., & Rabik, M. M. (2018). Multi criteria decision making of abrasive flow oriented process parameters in abrasive water jet machining using taguchi–DEAR Methodology. *Silicon*, *10*, 2015-2021. doi:10.1007/s12633-017-9715-x

Okponyia, K.O., & Oke, S.A. (2021). Novel EDAS-Taguchi and EDAS-Taguchi-Pareto methods for wire EDM process parametric selection of Ni55.8Ti (nitinol) shape memory alloy. *International Journal of Industrial Engineering and Engineering Management*, *3*(2), 105-122. doi:10.24002/ijieem.v3i2.4998

Perec, A., & Musial, W. (2021). Multiple Criteria Optimization of Abrasive Water Jet Cutting Using Entropy-VIKOR Approach. In: S. Hloch, D. Klichová, F. Pude, G. M. Krolczyk & S. Chattopadhyaya (Eds.), *Advances in Manufacturing Engineering and Materials II* (pp. 50-62). Springer. doi:10.1007/978-3-030-71956-2_5

Perec, A., Musial, W., Prazmo, J., Sobczak, R., Radomska-Zalas, A., Fajdek-Bieda, A., Nagnajewicz, S., & Pude, F. (2021). Multi-criteria Optimization of the Abrasive Waterjet Cutting Process for the High-Strength and Wear-Resistant Steel Hardox®500. In: D. Klichová, L. Sitek, S. Hloch & J. Valentinčič (Eds.), *Advances in Water Jetting* (pp. 145-154). Springer. doi:10.1007/978-3-030-53491-2_16

Perumal, A., Azhagurajan, A., Kumar, S.S., Kailasanathan, C., Rajan, R.P., Rajan, A.J., Venkatesan, G., & Rajkumar, P.R. (2020). Experimental investigation on surface morphology and parametric optimization of Ti-6Al-2Sn-4Zr-2Mo alpha beta alloy through AWJM.*Tierarztliche Praxis*, *40*, 1681-1702.

Perumal, A., Azhagurajan, A., Kumar, S. S., Prithivirajan, R., Baskaran, S., Rajkumar, P. R., Kailasanathan C., & Venkatesan, G. (2021). Influence of optimization techniques on wire electrical discharge machining of Ti–6Al–2Sn–4Zr–2Mo alloy using modeling approach. *Journal of Inorganic and Organometallic Polymers and Materials*, *31*, 3272-3289. doi:10.1007/s10904-021-01953-y

Perumal, A., Kailasanathan, C., Stalin, B., Kumar, S. S., Rajkumar, P. R., Gangadharan, T., Venkatesan, G., Nagaprasad, N., Dhinakaran, V., & Krishnaraj, R. (2022). Multiresponse optimization of wire electrical discharge machining parameters for Ti-6Al-2Sn-4Zr-2Mo (α-β) alloy using taguchi-grey relational approach. *Advances in Materials Science and Engineering*, *2022*, 6905239. doi:10.1155/2022/6905239

Pradhan, S., & Maity, K. (2018). Optimization of machining parameter characteristics during turning of Ti-6Al-4V using desirability function analysis. *Materials Today: Proceedings*, *5*(11-3), 25740-25749. doi:10.1016/j.matpr.2018.11.094

Singh, H., Bhoi, N.K., & Jain, P.K. (2021). Developments in abrasive water jet machining process-from 1980-2020. In: K. Gupta & A. Pramanik (Eds.), *Advanced Machining and Finishing, Handbooks in Advanced Manufacturing* (pp. 217-252). doi:10.1016/B978-0-12-817452-4.00011-7

Sitek, L., Hlaváček, P., Foldyna, J., Jarchau, M., & Foldyna, V. (2021). Pulsating abrasive water jet cutting using a standard abrasive injection cutting head – preliminary tests. In: D. Klichová, L. Sitek, S. Hloch & J. Valentinčič (Eds.), *Advances in Water Jetting* (pp. 186-196). Springer. doi:10.1007/978-3-030-53491-2_20

Ulutas, A. (2017) Sewing machine selection for a textile workshop by using EDAS method. *Journal of Business Research Turk*, *9*(2), 169-183.

Wang, S., Yang, F., Hu, D., Tang, C., & Lin, P. (2021). Modelling and analysis of abrasive water jet cutting front profile. *The International Journal of Advanced Manufacturing Technology*, *114*, 2829-2837. doi:10.1007/s00170-021-07014-5

Zohoor, M., & Nourian, S.H. (2012). Development of an algorithm for optimum control process to compensate the nozzle wear effect in cutting the hard and tough material using abrasive water jet cutting process. *The International Journal of Advanced Manufacturing Technology*, *61*, 1019-1028. doi:10.1007/s00170-011-3761-0